HEALTH AND MEDICINE

In situ repair abilities of human umbilical cord–derived mesenchymal stem cells and autocrosslinked hyaluronic acid gel complex in rhesus monkeys with intrauterine adhesion

Lingjuan Wang*, Chuanhu Yu*, Tianli Chang*, Mengdi Zhang, Su Song, Chengliang Xiong, Pin Su†, Wenpei Xiang†

Increasing occurrence of moderate to severe intrauterine adhesion (IUA) is seriously affecting the quality of human life. The aim of the study was to establish IUA models in nonhuman primates and to explore the dual repair effects of human umbilical cord–derived mesenchymal stem cells (huMSCs) loaded on autocrosslinked hyaluronic acid gel (HA-GEL) on endometrial damage and adhesion. Here, we recorded the menstrual cycle data in detail with uterine cavities observed and endometrial tissues detected after intervention, and the thicker endometria, decreased amount of fibrotic formation, increased number of endometrium glands, etc., suggested that both HA-GEL and huMSC/HA-GEL complexes could partially repair IUA caused by mechanical injury, but huMSC/HA-GEL complex transplantation had notable dual repair effects: a reliable antiadhesion property and the promotion of endometrial regeneration.

INTRODUCTION

Intrauterine adhesion (IUA), known as Asherman syndrome, is described as the partial or complete binding of the uterine cavity due to the buildup of scar tissue formation in the upper functional layer, resulting from endometrial damage to the lower basal layer (*1*). Repeated intrauterine operations, such as dilatation and curettage (D&C) and hysteroscopy, are the main cause of the common prevalence of IUA, with approximately 45% of moderate-to-severe cases occurring in these circumstances (*2*). Severe endometrium dysfunction will cause women within reproductive age to have this reproductive disadvantage, which was once considered a "terminal disease" that caused infertility (*3*, *4*).

Therefore, the vital aim for IUA treatment is to re-establish the uterine cavity and restore endometrial function. The current and standard operation method for IUA is hysteroscopic transcervical resection of adhesion (TCRA), while the preferred alternative involves the combined application of various adjuvant therapies, including physical barriers (contraceptive device, intrauterine balloon device, Foley balloon, etc.) for postoperative adhesion and estrogen therapy and amnion graft for endometrial regeneration (*5*–*8*). Although there is a certain therapeutic efficacy of these antiadhesion strategies, there are some disadvantages and shortcomings to the strategies that cannot be ignored, such as resistance to secondary surgery, limited area of isolation, induction of intrauterine inflammatory response, and difficulty in endometrial regeneration (*9*). Further, the high recurrence rate of postoperative adhesion and the low clinical pregnancy rate are still a focus and are universally recognized as a problem for patients with severe IUAs (*4*, *10*).

Autocrosslinked hyaluronic acid gel (HA-GEL), another promising physical barrier with natural mix of extracellular matrix and synovial fluid, has been approved by China Food & Drug Administration (CFDA) as a medical device for clinical practice after hysteroscopic adhesiolysis to achieve improvement in histocompatibility and viscosity, and the American Association of Gynecologic Laparoscopists has reported the effectiveness of HA-GEL in the prevention of IUAs in 2017 (*11*). The application of HA-GEL in uterine cavity treatment has its own advantages of few degradations by product retention following the outflow of menstrual blood (*11*, *12*). Compared to the previously used biomaterials, HA-GEL has a prolonged absorption time (as long as 7 to 14 days), the expansion characteristics of which can continuously isolate the postoperative uterine cavity to resist adhesion recurrence, and its other material properties can regulate the inflammatory response and repair endometrial injuries. Related experimental and clinical studies have suggested that HA-GEL is effective in the prevention of postoperative adhesion, and when combined application with a TCRA operation, it showed increases (~58.5%) in the effective rate of postoperative antiadhesion and decreases (~66.1%) in the postoperative recurrence rate (*13*). However, for severe IUA with a seriously injured basal layer and a loss of functional endometrium, endometrial regeneration remains an enormous challenge owing to the limited efficacy of current interventions.

Recently, stem cell–based therapy has emerged as a promising and exciting method of tissue regeneration (*14*–*16*). Human umbilical cord–derived mesenchymal stem cells (huMSCs) originate from the embryonic mesoderm and have the potential for multipotent differentiation; they have been regarded as a promising and extensive source for cell-based therapies due to their easy collection from discarded umbilical cords and their low immunogenicity. Some studies have shown the potential of huMSCs to repair damaged tissue (*17*–*20*), and the feasibility of stem cells in restoring the endometrial structure and function has also been verified by additional clinical and experimental studies (*21*–*24*). In this study, we used rhesus monkeys to construct a previously unidentified animal model of IUA and aimed to develop a complex of huMSCs loaded on HA-GEL to increase the local perseverance and activity of the stem cells and to improve the

Institute of Reproductive Health, Center of Reproductive Medicine, Tongji Medical College, Huazhong University of Science and Technology, Wuhan, China.
*These authors contributed equally to this work.
†Corresponding author. Email: wpxiang2010@gmail.com (W.X.); suping24@126.com (P.S.)

poor prognosis with the following dual functions: preventing postoperative adhesion with biomaterials and repairing the full layer of uterine wall. We also aimed to analyze the related repair or endometrial injuries, to study the motivation behind endometrial regeneration, and to explore the underlying mechanisms.

RESULTS

Phenotype characterization of huMSCs and their safety assessment and verification on HA-GEL

huMSCs [passage 3 (P3) to P9] had an appearance that was similar to typical spindle-shaped fibroblast-like cells, and they were arranged closely with vortex-like growth (fig. S1A1). The positive cells that were expanded in the enriching culture were successfully induced to become osteoblasts with bone matrix formation and adipocytes with lipid droplet formation (fig. S1A2 and A3). In addition, fluorescence-activated cell sorting (FACS) showed that the targeted cells expressed CD44 (99.40%), CD73 (99.56%), CD90 (99.92%), and CD105 (99.80%), but not CD34, CD45, and HLA-DR (<1%; fig. S1B).

To further evaluate the safety of huMSCs on HA-GEL, FACS results preliminarily verified that there was a low parentage of apoptotic cells in the coculture group (huMSCs/HA-GEL), and there was no notable difference between the coculture group and the culture-separated group (huMSCs) (fig. S2, A to C). In addition, the live-dead cell staining result we obtained before was added, and the result showed a small number of dead cells in both the huMSCs/HA-GEL and huMSCs groups, without significant difference compared with that in the culture-separated group (huMSCs) (fig. S2, D and E).

Establishment of IUA models with the evaluation of relevant morphological and histopathological parameters

Two months after endometrial intervention by uterine D&C, all six monkeys stopped menstruating; smaller uterine cavities and pale and uneven endometrial surfaces were observed, which had an adhesive zone full of endometrial cavity fluid. Thinner endometrial tissue was detected and observed under Doppler ultrasound scanning with discontinuous endometria and strong echo (Fig. 1A), and the endometrial thickness (1.9833 ± 0.4298 mm) after mechanical injury showed significant differences when compared with the thickness (4.0333 ± 0.5185 mm) before intervention ($P < 0.01$, $n = 6$; Fig. 1B and table S1). Changes in the structure of the endometrial tissues were assessed by hematoxylin and eosin (H&E) staining. Two months after mechanical injury, the endometrium was disorganized and had few or no glands (Fig. 1C). Endometrial gland numbers decreased markedly compared with those of the premechanical injury (0.6839 ± 0.8608 versus 6.8576 ± 2.6901 per unit area, respectively) ($P < 0.001$, $n = 6$; Fig. 1D and table S1). Similarly, to further evaluate the degree of fibrosis, Masson staining was performed at 2 months after mechanical injury (Fig. 1E). Increased fibrotic area ratios were detected and were analyzed quantitatively; more collagen deposition was observed at 2 months after mechanical injury compared with that of the premechanical injury (0.6557 ± 0.6359% versus 0.0716 ± 0.0942%) ($P < 0.05$, $n = 6$; Fig. 1F and table S1).

The intrauterine effect of huMSCs on HA-GEL

Two months after the huMSCs/HA-GEL complex was transplanted into the uterine cavity, menstruation resumed cycling in all monkeys, and there were significantly more endometrial gland numbers (4.9662 ± 1.4935, per unit area) than there were (3.6320 ± 1.0060, per unit area) after HA-GEL transplantation alone ($P < 0.01$; Fig. 2, A and B, and table S2). Moreover, the huMSCs/HA-GEL transplantation group showed marked decreases in fibrotic areas (5.5955 ± 3.6572%) compared with that of the HA-GEL transplantation group (14.2131 ± 13.7193%) ($P < 0.01$; Fig. 2, C and D, and table S2).

Abdominal surgeries were carried out, and three normal uterine cavities were exposed and revealed a thicker endometrium without an adhesive zone and endometrial cavity fluid in the huMSCs/HA-GEL transplantation group, whereas three uterine cavities in the HA-GEL transplantation group were still found to be abnormal with a mild to moderate amount of adhesion and a thinner rough endometrium (Fig. 3A). In addition, the smooth and thicker endometrial tissue with a third-line echo was also revealed and verified by ultrasound examination in the huMSCs/HA-GEL transplantation group (Fig. 3B), and the endometrial thickness (4.2667 ± 0.5558 mm) was significantly different compared with that (1.0667 ± 0.6650 mm) in the HA-GEL transplantation group ($P < 0.01$; Fig. 3C and table S2). Furthermore, the ultrastructure of the endometrium in the huMSCs/HA-GEL transplantation group showed short and sparse microvilli on the surface of epithelial cells, mucinous secretions in the glandular cavity with orderly arranged cells, tight intercellular junctions, and obvious edema of stroma, but the endometrial ends were uneven and the cellular edges had a frayed morphology. Further, loose connections between cells were observed in the HA-GEL transplantation group (Fig. 3D).

By systematic and comprehensive comparison of endometrial tissues before surgery, increased gland numbers were found both in the HA-GEL transplantation group (3.63 ± 1.01 versus 0.68 ± 0.86, respectively, per unit area; $P < 0.001$) and in the huMSCs/HA-GEL transplantation group (4.97 ± 1.49 versus 0.68 ± 0.86, respectively, per unit area; $P < 0.001$). The gland numbers were approaching normal levels (6.86 ± 2.69, per unit area; pre-D&C) 2 months after huMSCs/HA-GEL transplantation (Fig. 4A and table S3). Conversely, the Masson staining showed an increasing degree of fibrotic aggravation 2 months after HA-GEL transplantation (14.21 ± 13.72% versus 0.66 ± 0.64%; $P < 0.05$), but there was only a slight increase in fibrosis and some relief of aggravation after transplantation of the huMSCs/HA-GEL complex (5.60 ± 3.66 versus 0.66 ± 0.64; $P < 0.01$) (Fig. 4B and table S3). There was no significant difference in endometrial thickness or after mechanical injury (1.07 ± 0.67 versus 1.98 ± 0.41 mm) 2 months after HA-GEL transplantation compared with that of the HA-GEL transplantation, while the endometrial thickness was notably increased after transplantation of the huMSCs/HA-GEL complex (4.27 ± 0.56 versus 1.98 ± 0.41 mm; $P < 0.01$) that was similar to the normal levels observed before mechanical injury of the endometria (4.03 ± 0.52 mm; pre-D&C) (Fig. 4C and table S3).

The endometrial localization of huMSCs and the evidence of paracrine effects from co-transplanted huMSCs

The probe "Vysis SRY Probe LSI SRY Spectrum Orange/Vysis CEP X Spectrum Green" was used to mark huMSCs by a fluorescence in situ hybridization (FISH) technique. However, it was unclear if there was homology of probe sequences for the Yp11.3 region [sex-determining region Y (*SRY*), associated probe sequence] and *DXZ1* (Xp11.1-Xq11.1) (CEP X, associated probe sequence) between human and rhesus monkeys. By directly extracting DNA from huMSCs (containing XY chromosome) and the spleens of rhesus monkeys, it

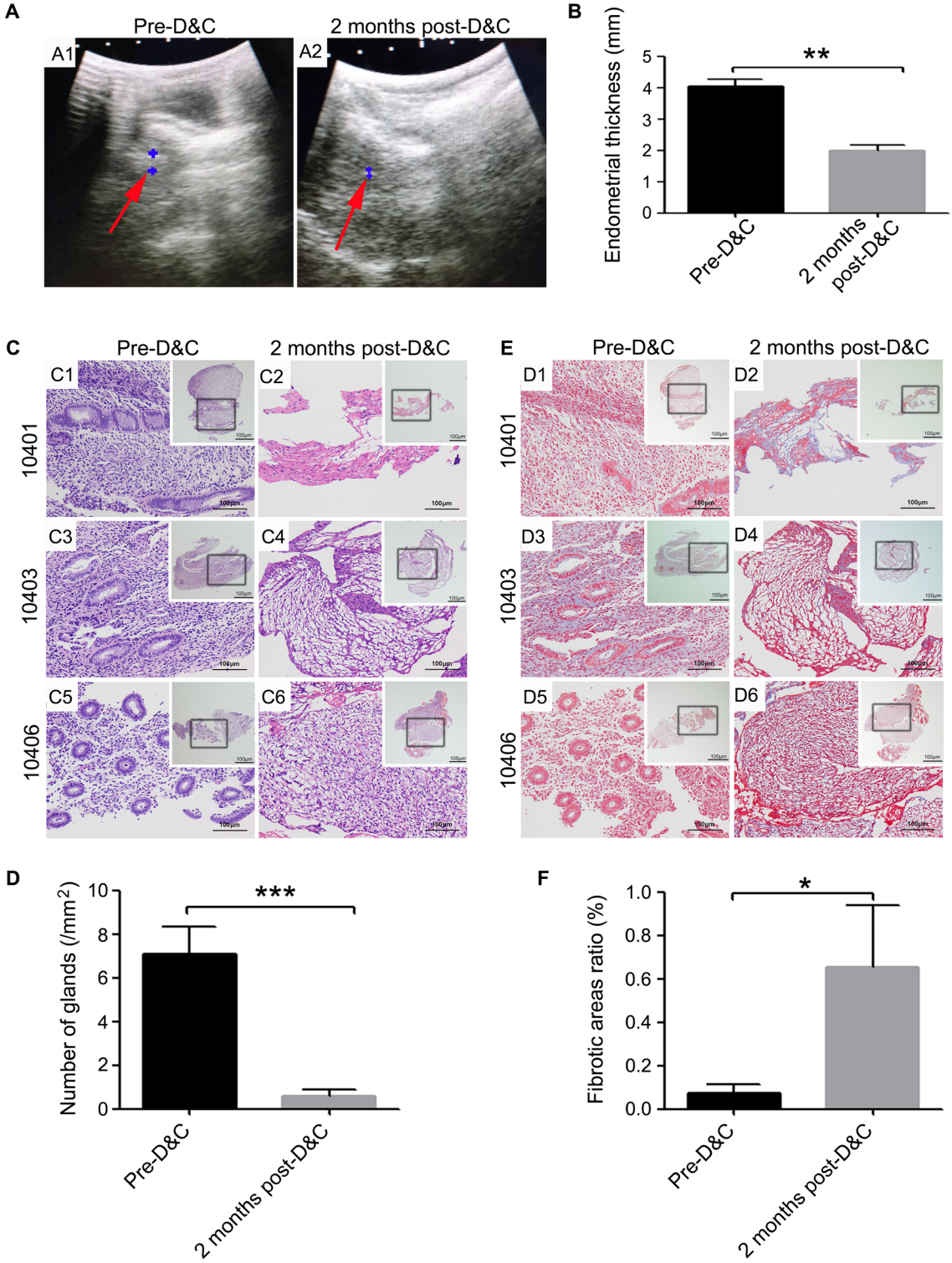

Fig. 1. The evaluation of IUA model establishment. (**A**) Detection of Doppler ultrasound. A1: Representative image of endometrial thickness for pre-D&C; A2: Representative image of endometrial thickness at 2 months post-D&C (red arrow, the endometrium echo; blue area, the largest cross section of endometrium). (**B**) Comparisons of endometrial thickness for pre- or post-D&C. (**C**) H&E staining of endometria for pre-D&C (C1, C3, and C5) and post-D&C (C2, C4, and C6); 10401, 10403, and 10406, respectively; see table S3 for details. Inserted overview pictures are of lower magnification; black squares are highly magnified regions. (**D**) Masson staining of endometria for pre-D&C (D1, D3, and D5) and post-D&C (D2, D4, and D6); 10401, 10403, and 10406, respectively; see table S3 for details. Inserted overview pictures are of lower magnification; black squares are highly magnified regions. (**E**) Comparisons of endometrial gland numbers per unit area for pre- or post-D&C. (**F**) Comparisons of fibrotic area ratios for pre- or post-D&C. *$P < 0.05$, **$P < 0.01$, and ***$P < 0.001$ versus the pre-D&C group, and the results shown are the mean ± SEM of three technical replicates from each animal.

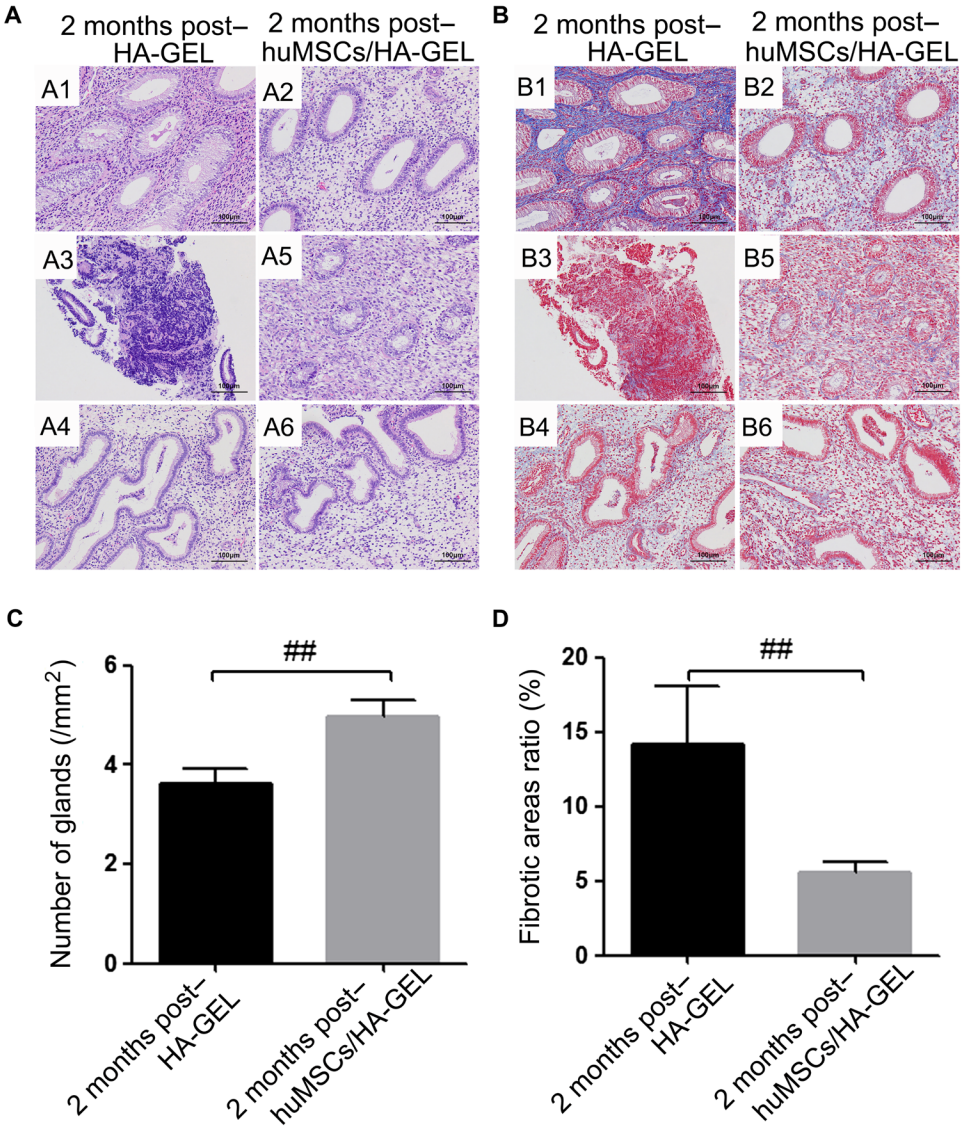

Fig. 2. Histological inspection of different interventions. (**A**) Endometrial H&E staining at 2 months after HA-GEL transplantation (A1, A3, and A4 correspond to 10401, 10403, and 10404, respectively) and huMSCs/HA-GEL transplantation (A2, A5, and A6 correspond to 10402, 10405, and 10406, respectively); 10401 to 10406, see table S3 for details. (**B**) Endometrial Masson staining at 2 months after HA-GEL transplantation (B1, B3, and B4 correspond to 10401, 10403, and 10404, respectively) and huMSCs/HA-GEL transplantation (B2, B5, and B6 correspond to 10402, 10405, and 10406, respectively); 10401 to 10406, see table S3 for details. (**C**) Comparisons of endometrial gland numbers per unit area between the HA-GEL transplantation group and the huMSC/HA-GEL transplantation group. (**D**) Comparisons of fibrotic area ratios between the HA-GEL transplantation group and the huMSCs/HA-GEL transplantation group. $^{\#\#}P < 0.01$ versus HA-GEL transplantation group, and the results shown are the mean ± SEM of three technical replicates from each animal.

was verified that the two probe sequences did not share homology between human and rhesus monkey (fig. S3). Then, human endometrial tissue was obtained as a positive control group (Fig. 5A), and one of the three endometria in the HA-GEL transplantation group was randomly selected as a negative control (Fig. 5B). FISH detection showed the absence of a positive signal (green/orange double signal or green signal) in the endometria 2 months after huMSCs/HA-GEL transplantation (Fig. 5, C to E), suggesting that huMSCs failed to locate to the endometrium after transplantation into the uterine cavity.

Furthermore, potential cytokines secreted by huMSCs were further detected in the endometria by immunofluorescence staining, and as expected, increased positive expression was found in the endometria of the huMSCs/HA-GEL transplantation group; there were significant differences in insulin-like growth factor (IGF-1), epidermal growth factor (EGF), and brain-derived neurotrophic factor (BDNF) between the two transplanted groups ($P < 0.05$), but there were no significant differences in vascular endothelial growth factor (VEGF) and hepatocyte growth factor (HGF) (Fig. 6, A and B). In addition, when compared with the HA-GEL transplantation group, the expression levels of proinflammatory cytokines [interferon-γ (*IFN*-γ)] were significantly decreased in the huMSCs/HA-GEL transplantation group ($P < 0.01$, Fig. 6C1), and significantly up-regulated expression was found for the anti-inflammatory cytokine [interleukin 4

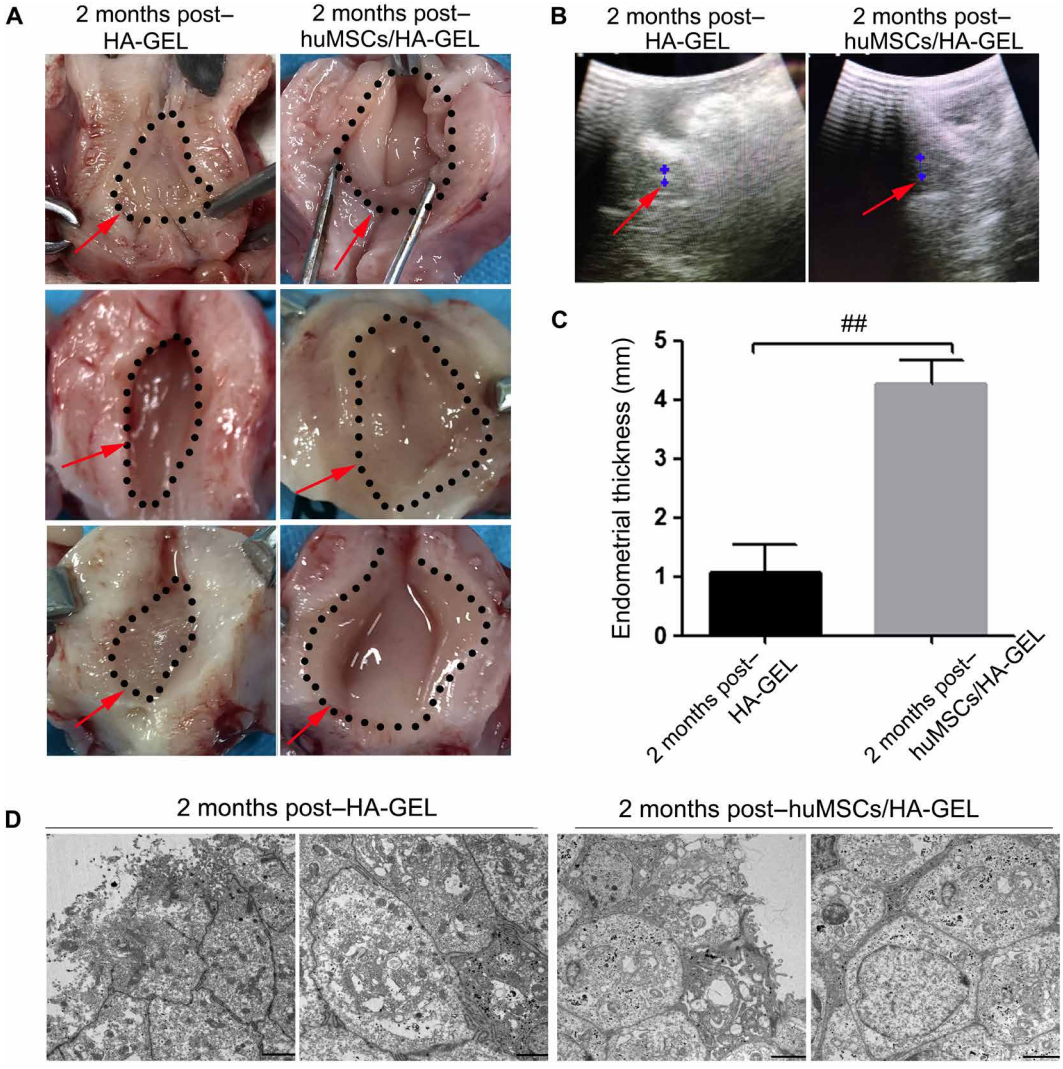

Fig. 3. The endometrial effects of different interventions on morphology and ultrastructure. (**A**) Representative images of uterine cavities in the HA-GEL transplantation and huMSCs/HA-GEL transplantation groups (the dotted area and the red arrow mark the endometrial area). (**B**) Representative images of endometrial thickness for ultrasound detection in the HA-GEL transplantation and huMSCs/HA-GEL transplantation groups (the red arrow marks the endometrial echo; the blue area marks the largest cross section of the endometrium). (**C**) Comparisons of endometrial thickness between the HA-GEL transplantation group and the huMSCs/HA-GEL transplantation group. (**D**) Representative images of ultrastructural changes in the HA-GEL transplantation and huMSCs/HA-GEL transplantation groups (the left panel shows the surface of epithelial cells; the right panel shows the intercellular changes). $^{\#\#}P < 0.01$ versus 2 months post–HA-GEL, and the results shown are the mean ± SEM of three technical replicates from each animal. Photos provided by Lingjuan Wang and Chengliang Xiong (Institute of Reproductive Health, Center of Reproductive Medicine, Tongji Medical College, Huazhong University of Science and Technology).

(*IL-4*)] ($P < 0.01$, Fig. 6C2), as well as related cytokines that promote cell proliferation and tissue repair (*IGF-1* and *EGF*) ($P < 0.001$, $P < 0.05$, respectively; Fig. 6, C3 and C4).

DISCUSSION

At present, according to relevant reports, approximately 2.8 to 45.5% of women with impaired fertility suffer from IUA, and more than 90% of cases occur after pregnancy-related D&C (*25*). In this study, an IUA model was successfully established with an invasive surgery in nonhuman primates (rhesus monkeys), which have a genetic background, endocrine system, menstrual cycle, and anatomical structure that are similar to humans (*26*). This model allowed us to further explore new approaches for the intervention and treatment of adhesion, especially the thin endometrium caused by endometrial injury.

In the primate experiments, 6- to 7-year-old rhesus monkeys (reproductive age) were identified as the ideal subjects for establishing IUA models; they had regular menstrual cycles of approximately 21 to 30 days, which was observed and recorded in succession for the 2 months before mechanical injury. We developed the first model of endometrial injury in rhesus monkeys by open abdominal surgery; we verified the successful establishment by visualizing the hard and narrow cervix and confirmed that D&C could ultimately lead to severe IUA, which was characterized by severe endometrial fibrosis, loss of normal endometrial glands, paper-thin and discontinuous

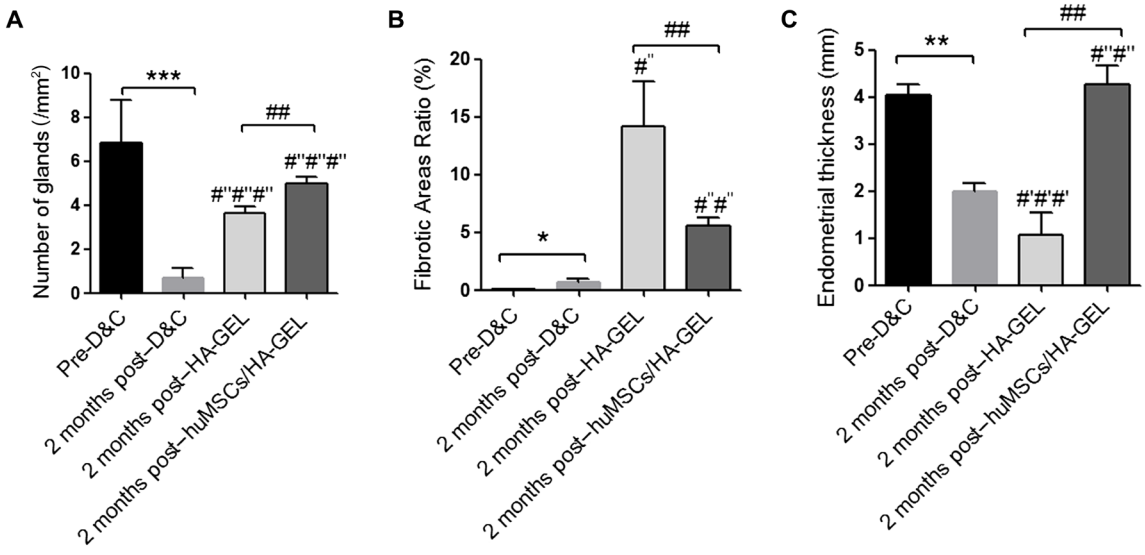

Fig. 4. Comprehensive assessment for the effects of different interventions on endometrial regeneration and remodeling. (**A**) Comparisons of endometrial gland numbers per unit area. (**B**) Comparisons of ratios of fibrotic area (%). (**C**) Comparisons of endometrial thickness (mm). $^{*}P < 0.05$, $^{**}P < 0.01$, and $^{***}P < 0.001$, all versus pre-D&C; $^{\#'\#'\#'}P < 0.001$ versus pre-D&C; $^{\#''}P < 0.05$, $^{\#''\#''}P < 0.01$, and $^{\#''\#''\#''}P < 0.001$, all versus 2 months post-D&C; $^{\#\#}P < 0.01$ versus 2 months post–HA-GEL, and the results shown are the mean ± SEM of three technical replicates from each animal.

endometria, full of adhesive zone and endometrial cavity fluid, as well as amenorrhea, as noted by the American Fertility Society scoring method (*27*).

This study explored the effect of transplantation huMSCs combined with HA-GEL on intrauterine reconstruction and endometrial regeneration in an IUA model. In our study, when compared with the control group (transplantation of only HA-GEL), the effects of the group with huMSCs were confirmed by Doppler ultrasonic scanning, histological inspection, and ultrastructure detection 2 months after transplantation. In the experimental group, the injured endometrial tissue presented with a thicker endometrium, an increased number of endometrial glands, a decreased fibrotic area, and typical changes in the secretory phase, showing how the positive huMSCs acted upon endometrial repair and regeneration through secreting cytokines and growth factors (*16*); further, the HA-GEL acted as a physical barrier to severe adhesion and provided an ideal physical support for the attachment of huMSCs to prevent their rapid outflow from uterine cavity.

Specifically, in the control group (HA-GEL transplanted alone), subjects did not recover menstruation and normal uterine cavity. However, recovery of menstruation, the appearance of a normal uterine cavity, and normal cycling were observed in the other three rhesus monkeys 2 months after huMSCs/HA-GEL co-transplantation, suggesting the great effect of the huMSCs/HA-GEL complex on the reconstruction of the uterine cavity and on the blocking of adhesion. Meanwhile, we also found that HA-GEL transplantation could increase the number of endometrial glands, but it played no effective role in endometrial thickness, which was important because it was less effective than the huMSCs/HA-GEL complex. This amelioration of the damage to the endometria resulted in nearly normal levels and suggested the re-emergence of endometrial repair and regeneration after huMSCs/HA-GEL co-transplantation. In addition, the degree of fibrosis in the damaged endometria was found to be increasingly worse 2 months after transplantation despite HA-GEL or huMSCs/HA-GEL intervention, and it remained unclear whether HA-GEL had an effect on resisting fibrogenesis because of the small sample size of rhesus monkeys. Obviously, huMSCs/HA-GEL intervention relieved the worse aspects of fibrogenesis, suggesting a better outcome and potential effect on the reconstruction of abnormal tissue.

Then, it was unclear what the underlying mechanism of endometrial reconstruction was. Transplanted huMSCs were tracked in endometria, and the result showed no obvious labeled signal in endometrial tissue at 2 months after huMSCs/HA-GEL complex transplantation, which was contrary to a previous report (*28*, *29*). To explain these conflicting results, three possibilities were proposed: (i) missed target area due to random sampling, (ii) completely eliminated following the outflow of menstrual blood, and (iii) huMSC apoptosis and depletion. However, the last two assumptions were preferred for the reason of multipoint sampling and continuous paraffin section, and if the endometrial tissues were obtained at 1 week or 2 weeks after huMSCs/HA transplantation, we might get different results owing to the similar menstrual cycles to human and different physiological function from animal models such as mice and rabbits. Alternatively, some cytokines and growth factors related to huMSCs were detected, and the results showed that huMSCs/HA-GEL complex transplantation could obviously increase the expression of IGF-1, EGF, BDNF, and so on compared to that of the control group (HA-GEL transplanted alone). Growth factors and their related peptides were deemed to mediate and regulate hormones working on target tissues through autocrine or paracrine function, and some growth factors, the endocrine basis of endometrium recycling including transforming growth factor, EGF, IGF, fibroblast growth factor, etc., were reported to regulate the differentiation and proliferation of endometrial cells (*30*). EGF, present in stromal and epithelial cells of the endometrium, could regulate endometrial proliferation, gland secretion, and decidual transformation (*31*). IGF played important roles in endometrial physiology and could regulate the cell cycle

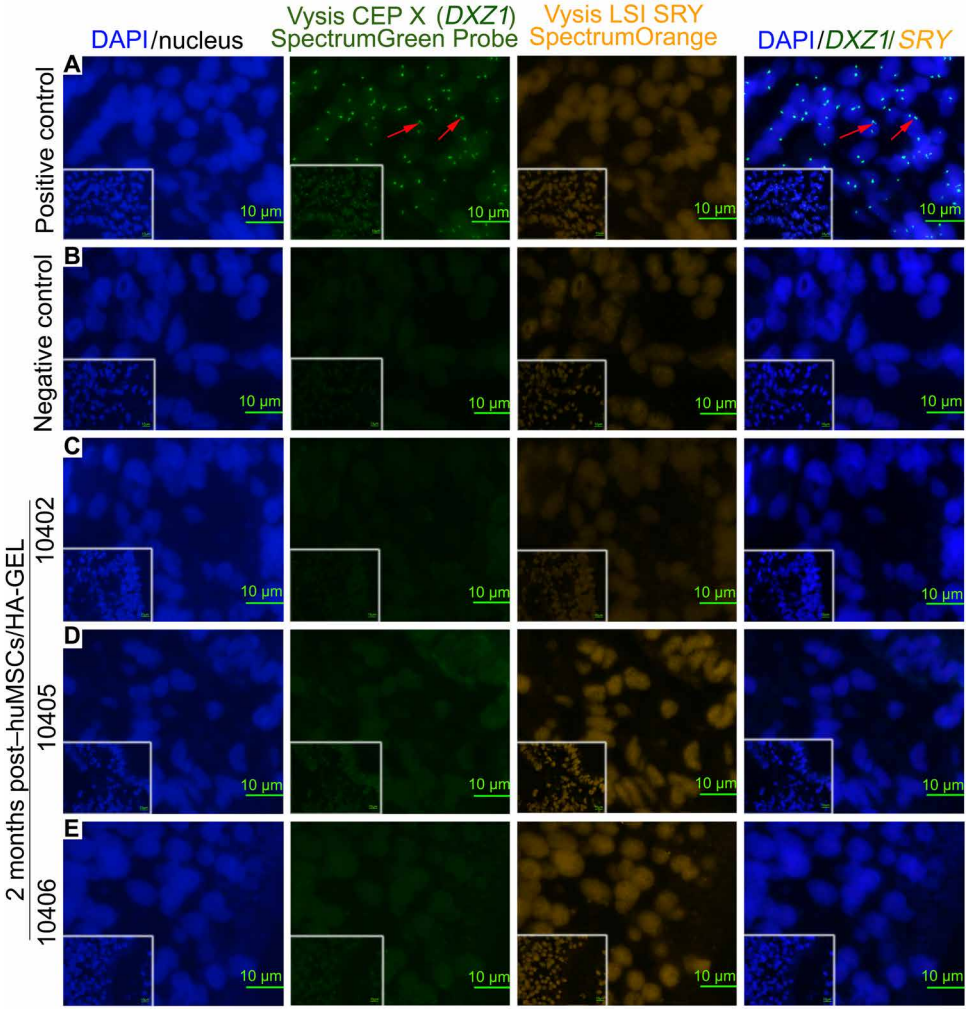

Fig. 5. FISH analysis for tracking transplanted huMSCs in the endometrium. (**A**) Positive control, human endometrium (containing XX chromosomes); the red arrow indicates the green signal for Vysis CEP X (*DXZ1*). (**B**) Endometrial localization of huMSCs in the HA-GEL transplantation group (negative control). (**C** to **E**) Distribution of huMSCs in endometria 2 months after huMSCs/HA-GEL co-transplantation. Double/single-labeled staining (orange/green signal or just green signal) cells were defined as huMSCs. For details on 10402, 10405, and 10406, see table S3. Inserted overview pictures show a lower magnification.

and promoted the proliferation of endometrial epithelial cells after the activation of estrogen (*32*, *33*). Moreover, some reports showed the key role of BDNF in the regulation of endometrial cell proliferation by the downstream signal transducer and activator of transcription 3 signaling pathway and participating in the damage repair of endometrium (*34*, *35*). Furthermore, considering the effect of huMSCs on uncontrolled fibrogenesis resulting from inflammatory activity and endometrial cell proliferation, anti-inflammatory cytokines (*IL-4*) were observed to be up-regulated, and proinflammatory cytokines (*IFN-γ*) were down-regulated; further, related cytokines that promote cell proliferation and tissue repair were up-regulated, such as *IGF-1* and *EGF*, suggesting that excessive fiber formation could be inhibited by anti-inflammatory effects due to the advantageous microenvironment constructed by abundant huMSCs in the uterine cavity. VEGF, as the most important vascular growth factor, could be stimulated by ischemia and hypoxia in the endometrial layer after endometrial injury and played an important role in the early stage of endometrial repair and proliferation; during the time, angiogenesis could be promoted rapidly, but no effects were shown once the neovascularization was over (*36*–*39*). We speculated that no difference found in VEGF expression might be related to the samples extracted from the endometrium during the secretory phase, a plateau stage of vascular repair and VEGF secretion in the endometrial basal layer. Overall, all of these results further verified the important role of huMSCs in damage repair by secreting a series of paracrine factors, such as anti-inflammatory factors, growth factors, and cytokines, related to constructing the microenvironment with properties such as anti-inflammatory, promoting repair, maintaining cell function, angiogenesis, etc., which was consistent with the previous report (*40*).

In conclusion, this study showed that both HA-GEL and huMSC/HA-GEL complexes could partially repair severe IUA caused by mechanical injury, but huMSC/HA-GEL complex transplantation indicated significant advantages in the dual repair effects of antiadhesive property and promotion of endometrial regeneration. By constructing a complex of huMSCs/HA-GEL with a biomaterial to prevent adhesion and allow stem cells to act at the appropriate site of repair of the endometrium, we have provided a method for solving a problem

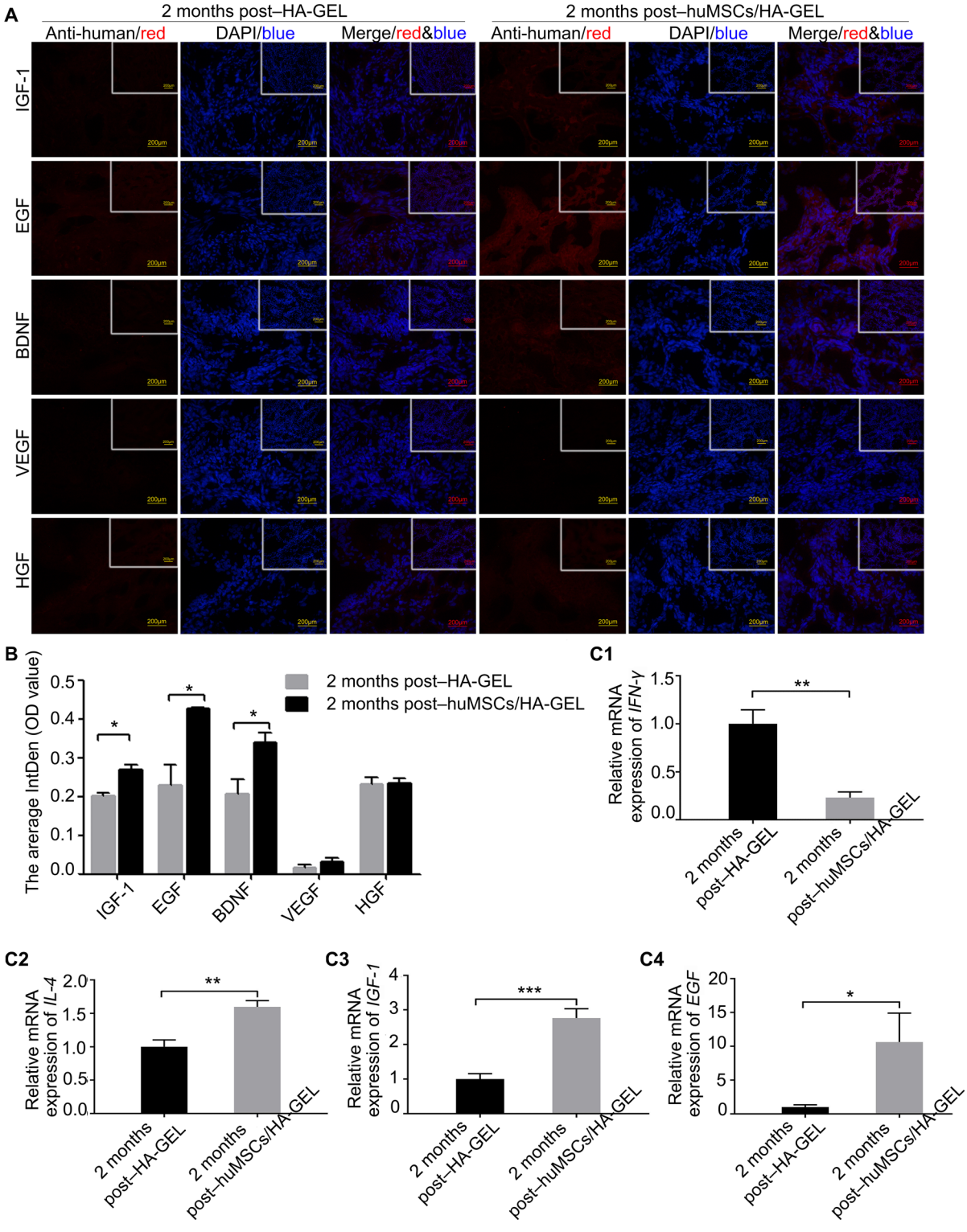

Fig. 6. The expression of cytokines in the endometria. (**A**) The expression and localization of the potential cytokines secreted by huMSCs in the HA-GEL transplantation group and the huMSCs/HA-GEL transplantation group; inserted overview pictures show a lower magnification. (**B**) The optical density (OD) value of IGF-1, EGF, BDNF, VEGF, and HGF 2 months after HA-GEL transplantation or huMSCs/HA-GEL co-transplantation. (**C1**) Comparison of *IFN-γ* mRNA expression between the HA-GEL transplantation group and the huMSC/HA-GEL transplantation group. (**C2**) Comparison of *IL-4* mRNA expression between the HA-GEL transplantation group and the huMSC/HA-GEL transplantation group. (**C3**) Comparison of *IGF-1* mRNA expression between the HA-GEL transplantation group and the huMSC/HA-GEL transplantation group. (**C4**) Comparison of *EGF* mRNA expression between the HA-GEL transplantation group and the huMSC/HA-GEL transplantation group. **P* < 0.05, ***P* < 0.01, and ****P* < 0.001 versus 2 months post–HA-GEL; the results shown are the mean ± SEM of three technical replicates from each animal.

for patients with moderate to severe IUA and thin endometria caused by IUA. We hope that this novel strategy using the huMSCs/HA-GEL complex will be offered as a basic clinical research strategy in the future, and it might be a potential valuable treatment for gel loaded with cytokines to repair moderate to severe IUA.

MATERIALS AND METHODS

Experimental animals

The basic information for the six rhesus monkeys used in this study is shown in table S4. They were bred and supplied by Fujian Experiment Center of Nonhuman Primate for Family Planning, where they were maintained the clean-class animal feeding standards. We used these rhesus monkeys in the study following the outlined steps of the flowchart (fig. S4) from 17 September 2018 to 16 March 2019 with regular menstrual cycle observed (*26*). All experiments were conducted in accordance with the National Research Council's "Guideline for the Care and Use of Laboratory Animals" and approved by the Ethics Committee of the Center of Reproductive Medicine of Tongji Medical College of Huazhong University of Science and Technology in China.

Establishment of IUA models

The six rhesus monkeys were chosen for IUA models following mechanical injury, and intraperitoneal surgery was the proper choice for curettage in view of the special structure of the vagina and the cervix, which are characterized by hardness, toughness, a small aperture, and a long cervix. All monkeys were provided general anesthesia with an appropriate dose of ketamine by intramuscular injection, and then a mid-abdominal longitudinal incision was made to expose the uterus. A vertical incision (~0.5 cm) was made in the lower uterine segment. A small curettage spoon was used to deeply scrape the uterine walls until they became rough and pale, and the collected endometrial tissues were stored at −80°C. Subsequently, the uterine and abdominal incisions were closed by continuous stitching with 6-0 Vicryl sutures and 3-0 silk absorbable sutures, respectively. After the operation, antibiotics were used to prevent infection, and observation on the first day after the operation showed that these rhesus monkeys were in good condition.

huMSC preparation and identification

huMSCs were kindly provided by the Stem Cell Laboratory of the Center of Reproductive Medicine (Tongji Medical College, Huazhong University of Science and Technology, China). Frozen huMSCs between P3 and P9 were freshly seeded in 10-cm culture dishes (1×10^6 cells per dish) in Iscove's modified Dulbecco's medium (IMDM, Genom, China) supplemented with 10% (v/v) fetal bovine serum (FBS, Gibco, USA), penicillin (100 U/ml), and streptomycin (100 mg/ml; Gibco, USA). Briefly, the phenotypes of huMSCs were specifically identified by FACS, and the osteogenic and adipogenic capacities of the mesenchymal stem cells were assessed with a MesenCult Osteogenic Stimulatory Kit (STEMCELL Technologies Inc., Canada) and a MesenCult Adipogenic Differentiation Kit (STEMCELL Technologies Inc., Canada). P3 to P9 were used for the experiments.

huMSCs, safety assessment, and verification on an HA-GEL

To further evaluate the safety of huMSCs on HA-GEL, we mixed huMSCs (1×10^5 to 2×10^5 per well) and 300 μl of HA-GEL [Con., 5 mg/ml; Bioregen, Co., Ltd., China, approved by CFDA as a medical device (no. 20153641542)] evenly with sterile syringes in 24-well plates and then added IMDM (Genom, China), including 10% (v/v) FBS (Gibco, USA), penicillin (100 U/ml), and streptomycin (100 mg/ml) (Gibco, USA). After co-culture for 48 hours, 0.8% collagenase type I supplemented with appropriate hyaluronidase was used to digest HA-GEL and release huMSCs, and FACS was chosen for the detection of cell apoptosis index in the coculture group (huMSCs/HA-GEL) and the culture-separated group (huMSCs), as well as live-dead cell detection with Live-Dead Cytotoxicity Assay Kit (MesGen Biotechnology, Shanghai).

The construction and transplantation of the huMSCs/HA-GEL complex

Briefly, 50 μl of huMSCs (1×10^7 to 2×10^7 cells) were injected into 200 μl of HA-GEL (Bioregen, Co., Ltd. China), and then they were immediately transplanted into the uterine cavity through the open abdominal cavity. At the same time, the uterine cavity in the negative control group was injected into 200 μl of HA-GEL following the same procedure that was used for the huMSC/HA-GEL transplantation group. All operations were performed under sterile conditions.

Doppler ultrasound scanning

The endometrial thickness (before mechanical injury or after surgery for 2 months) was measured by an abdominal two-dimensional ultrasound system (Medison SA-600 Ultrasound System, Korea) with 3.5-MHz pulse repetition frequency to evaluate the damage to the endometrium and the endometrial regeneration.

H&E staining

The scraped pieces of endometrium were fixed in 4% paraformaldehyde for 24 hours and then embedded in paraffin. Serial paraffin-embedded sections (4 μm) were obtained, sequentially dewaxed in xylene I and xylene II for 20 min each, and rehydrated in a series of ethanol solutions with a decreasing concentration (100% for 10 min, 100% for 10 min, 95% for 5 min, 90% for 5 min, 80% for 5 min, and 70% for 5 min). Then, the sections were rinsed in distilled water (three times, 5 min each). The sections were stained with an H&E solution (Servicebio, China) according to the manufacturer's instructions. After staining, endometrial morphologic features were observed, and the number of uterine glands per unit area was counted according to five randomly selected high-power fields of each slide.

Masson staining

The 4-μm paraffin sections of endometrium were dewaxed and rehydrated as described above and then were immersed in Masson A solution (Servicebio, China) overnight, which was followed by a brief wash under running water. Then, the sections were stained in a mixed solution of Masson A and Masson B (1:1, Servicebio, China) for 1 min, washed under running water, and placed in 1% hydrochloric acid alcohol for 10 s before they were washed again. Subsequently, sections were immersed in Masson D solution (Servicebio, China) for 6 min and then were stained in Masson E solution (Servicebio, China) for 1 min. The solution was then slightly drained, and the sections were placed directly in Masson F solution (Servicebio, China) for 2 to 30 s, and then they were rinsed in 1% glacial acetic acid for differentiation of the signals. Last, the sections were dehydrated in absolute ethyl alcohol, clarified in xylene for 5 min, and sealed in Permount Mounting Medium (Sinopharm Chemical Reagent Co., Ltd., China). Endometrial fibrosis was assessed according to five random

fields on each slide, and the fibrotic area ratios were calculated using Image-Pro Plus software (version 6.0).

Total DNA and mRNA extraction, relative qRT-PCRs, and agarose gel electrophoresis

The total DNA samples were extracted from spleen tissue of rhesus monkeys and huMSCs carrying XY or XX chromosomes with a TIANamp Genomic DNA Kit (Tiangen Biotech Co., Ltd., Beijing). mRNA samples were extracted from endometrial tissue, and cDNA was synthesized with a RevertAid First Strand cDNA Synthesis Kit (Thermo, USA). Subsequently, quantitative real-time polymerase chain reaction (qRT-PCR) was performed to verify the specific expression of the *DXZ1* gene on the X chromosome, *SRY* on the Y chromosome, and *IFN*-γ, *IL-4*, *IGF-1*, and *EGF* using StepOne and StepOnePlus Real-Time PCR Systems Version 2.3. The final reaction volume of 20 μl contained 10 μl of Bestar qPCR MasterMix (SYBR Green) (DBI Bioscience), 4 μl of DNA samples, 0.4 μl of forward/reverse primer (10 μM), and 5.2 μl of DNA/RNase-free double-distilled water (ddH_2O). Last, agarose gel electrophoresis was performed to verify the expression of *DXZ1* and *SRY* in the spleen and huMSC tissues. In addition, primer sequences used for *DXZ1* (Xp11.1-Xq11.1), *SRY* (Yp11.3 Region), *IFN*-γ, *IL-4*, *IGF-1*, and *EGF* are summarized in table S5.

FISH technique for endometrial tracking of huMSCs

FISH analysis was performed to trace huMSCs for 2 months after the huMSCs/HA-GEL complexes were transplanted into the uterine cavity. Endometrial tissue was collected and immediately fixed in 10% paraformaldehyde before paraffin embedding. A Vysis SRY Probe LSI SRY Spectrum Orange/Vysis CEP X Spectrum Green Kit (Abbott Laboratories, USA) was used to mark huMSCs in the endometrium. All paraffin sections were dewaxed, rehydrated, hybridized with the probe, and so on according to the probe's instructions; a final counterstaining of 4′,6-diamidino-2-phenylindole (DAPI) was added, and visualization took place with fluorescence microscopy (Nikon Eclipse Ci, Nikon DS-U3). The orange (*SRY*/Y chromosome) and/or green (*DXZ1*/X chromosome) signals were used to verify the presence or absence of huMSCs in the endometrium.

Immunofluorescence assays

The following factors were analyzed after transplantation of the huMSCs/HA-GEL complex: trophic factors (cytokines) that are secreted by huMSCs [according to relevant reports (*17*)], proinflammatory cytokines, anti-inflammatory cytokines, and related cytokines that promote cell proliferation and tissue repair. After fixation with 4% paraformaldehyde, paraffin embedding, and cutting 4-μm paraffin sections, the slides were immersed in xylene and rehydrated through incubation in a series of alcohol gradients. The following specific antibodies were applied to sections at 4°C overnight in humidified chambers: recombinant anti-BDNF antibody (EPR1292) (ab108319, Abcam), anti-VEGF antibody (C-1: sc-7269, Santa Cruz), anti–IGF-1 antibody (W18: sc-74116, Santa Cruz), anti-HGFa antibody (H-10: sc-374422, Santa Cruz), and anti-EGF antibody (F-9: sc-166779, Santa Cruz). Then, these sections were incubated with a Cy3-tagged secondary antibody for 1 hour at room temperature and were then rinsed in ddH_2O three times. Counterstaining was performed with DAPI for 5 min, and the fluorescence signal was detected under a fluorescence microscope (Nikon Eclipse Ci, Nikon DS-U3).

Statistical analysis

We collected three technical replicates from each animal and repeated the experiments at least three times. The data presented as the mean ± SEM were analyzed with Statistical Package for the Social Sciences Statistics 17.0. The normally distributed numerical variance was assessed by a *t* test with homogeneity of variance, and χ^2 tests were used to analyze the differences between two or more rates. The percentage of positive area after H&E staining and Masson staining was measured using ImageJ 1.43u (Wayne Rasband, National Institutes of Health, USA). Statistical significance was assumed for $P < 0.05$.

SUPPLEMENTARY MATERIALS

Supplementary material for this article is available at http://advances.sciencemag.org/cgi/content/full/6/21/eaba6357/DC1

View/request a protocol for this paper from *Bio-protocol*.

REFERENCES AND NOTES

1. E. A. Evans-Hoeker, S. L. Young, Endometrial receptivity and intrauterine adhesive disease. *Semin. Reprod. Med.* **32**, 392–401 (2014).
2. A. B. Hooker, M. Lemmers, A. L. Thurkow, M. W. Heymans, B. C. Opmeer, H. A. M. Brölmann, B. W. Mol, J. A. F. Huirne, Systematic review and meta-analysis of intrauterine adhesions after miscarriage: Prevalence, risk factors and long-term reproductive outcome. *Hum. Reprod. Update* **20**, 262–278 (2014).
3. E. J. Guo, J. P. W. Chung, L. C. Y. Poon, T. C. Li, Reproductive outcomes after surgical treatment of Asherman syndrome: A systematic review. *Best Pract. Res. Clin. Obstet. Gynaecol.* **59**, 98–114 (2019).
4. D. Yu, Y.-M. Wong, Y. Cheong, E. Xia, T.-C. Li, Asherman syndrome—One century later. *Fertil. Steril.* **89**, 759–779 (2008).
5. R. Zhu, H. Duan, L. Gan, S. Wang, Comparison of intrauterine suitable balloon and Foley balloon in the prevention of adhesion after hysteroscopic adhesiolysis. *Biomed. Res. Int.* **2018**, 1–6 (2018).
6. X. Yu, L. Yuhan, S. Dongmei, X. Enlan, L. Tinchiu, The incidence of post-operative adhesion following transection of uterine septum: A cohort study comparing three different adjuvant therapies. *Eur. J. Obstet. Gynecol. Reprod. Biol.* **201**, 61–64 (2016).
7. A. A. E. Orhue, M. E. Aziken, J. O. Igbefoh, A comparison of two adjunctive treatments for intrauterine adhesions following lysis. *Int. J. Gynaecol. Obstet.* **82**, 49–56 (2003).
8. X. Peng, T. Li, Y. Zhao, Y. Guo, E. Xia, Safety and efficacy of amnion graft in preventing reformation of intrauterine adhesions. *J. Minim. Invasive Gynecol.* **24**, 1204–1210 (2017).
9. U. Salma, M. Xue, A. S. Md Sayed, D. Xu, Efficacy of intrauterine device in the treatment of intrauterine adhesions. *Biomed. Res. Int.* **2014**, 589296 (2014).
10. C. M. March, Management of Asherman's syndrome. *Reprod. Biomed. Online* **23**, 63–76 (2011).
11. AAGL Elevating Gynecologic Surgery, AAGL practice report: Practice guidelines on intrauterine adhesions developed in collaboration with the European Society of Gynaecological Endoscopy (ESGE). *J. Minim. Invasive. Gynecol.* **14**, 695–705 (2017).
12. V. Mais, M. G. Cirronis, M. Peiretti, G. Ferrucci, E. Cossu, G. B. Melis, Efficacy of auto-crosslinked hyaluronan gel for adhesion prevention in laparoscopy and hysteroscopy: A systematic review and meta-analysis of randomized controlled trials. *Eur. J. Obstet. Gynecol. Reprod. Biol.* **160**, 1–5 (2012).
13. S. Xiao, Y. Wan, F. Zou, M. Ye, H. Deng, J. Ma, Y. Wei, C. Tan, M. Xue, Prevention of intrauterine adhesion with auto-crosslinked hyaluronic acid gel: A prospective, randomized, controlled clinical study. *Zhonghua Fu Chan Ke Za Zhi.* **50**, 32–36 (2015).
14. Z. Khan, J. M. Goldberg, Hysteroscopic management of Asherman's syndrome. *J. Minim. Invasive Gynecol.* **25**, 218–228 (2018).
15. C. A. Salazar, K. Isaacson, S. Morris, A comprehensive review of Asherman's syndrome: Causes, symptoms and treatment options. *Curr. Opin. Obstet. Gynecol.* **29**, 249–256 (2017).
16. V. B. R. Konala, M. K. Mamidi, R. Bhonde, A. K. Das, R. Pochampally, R. Pal, The current landscape of the mesenchymal stromal cell secretome: A new paradigm for cell-free regeneration. *Cytotherapy* **18**, 13–24 (2016).
17. S. Yamasaki, H. Mera, M. Itokazu, Y. Hashimoto, S. Wakitani, Cartilage repair with autologous bone marrow mesenchymal stem cell transplantation: Review of preclinical and clinical studies. *Cartilage.* **5**, 196–202 (2014).
18. K. Ma, S. Liao, L. He, J. Lu, S. Ramakrishna, C. K. Chan, Effects of nanofiber/stem cell composite on wound healing in acute full-thickness skin wounds. *Tissue Eng. Part A* **17**, 1413–1424 (2011).
19. M. Dadon-Nachum, O. Sadan, I. Srugo, E. Melamed, D. Offen, Differentiated mesenchymal stem cells for sciatic nerve injury. *Stem. Cell Rev. Rep.* **7**, 664–671 (2011).

20. R. J. Henning, Stem cells in cardiac repair. *Future Cardiol.* **7**, 99–117 (2011).
21. C. B. Nagori, S. Y. Panchal, H. Patel, Endometrial regeneration using autologous adult stem cells followed by conception by *in vitro* fertilization in a patient of severe Asherman's syndrome. *J. Hum. Reprod. Sci.* **4**, 43–48 (2011).
22. Y. Zhao, A. Wang, X. Tang, M. Li, L. Yan, W. Shang, M. Gao, Intrauterine transplantation of autologous bone marrow derived mesenchymal stem cells followed by conception in a patient of severe intrauterine adhesions. *Open J. Obstet. Gyn.* **3**, 377–380 (2013).
23. N. Singh, S. Mohanty, T. Seth, M. Shankar, S. Bhaskaran, S. Dharmendra, Autologous stem cell transplantation in refractory Asherman's syndrome: A novel cell based therapy. *J Hum Reprod Sci.* **7**, 93–98 (2014).
24. Y. Cao, H. Sun, H. Zhu, X. Zhu, X. Tang, G. Yan, J. Wang, D. Bai, J. Wang, L. Wang, Q. Zhou, H. Wang, C. Dai, L. Ding, B. Xu, Y. Zhou, J. Hao, J. Dai, Y. Hu, Allogeneic cell therapy using umbilical cord MSCs on collagen scaffolds for patients with recurrent uterine adhesion: A phase I clinical trial. *Stem Cell Res. Ther.* **9**, 192 (2018).
25. E. Dreisler, J. J. Kjer, Asherman's syndrome: Current perspectives on diagnosis and management. *Int. J. Womens Health* **11**, 191–198 (2019).
26. Y. Su, H. Pan, B. Pan, M. Lu, Observation, diagnosis and midwifery of anatomy and physiology of reproductive system in female macaques. *Experimental animal science at Shanghai* **8**, 141–142 (1988).
27. Revised American Society for Reproductive Medicine classification of endometriosis: 1996. *Fertil. Steril.* **67**, 817–821 (1997).
28. L. Xin, X. Lin, Y. Pan, X. Zheng, L. Shi, Y. Zhang, L. Ma, C. Gao, S. Zhang, A collagen scaffold loaded with human umbilical cord-derived mesenchymal stem cells facilitates endometrial regeneration and restores fertility. *Acta Biomater.* **92**, 160–171 (2019).
29. L. Gan, H. Duan, Q. Xu, Y.-Q. Tang, J.-J. Li, F.-Q. Sun, S. Wang, Human amniotic mesenchymal stromal cell transplantation improves endometrial regeneration in rodent models of intrauterine adhesions. *Cytotherapy* **19**, 603–616 (2017).
30. M. E. Sak, T. Gul, M. S. Evsen, H. E. Soydinc, S. Sak, A. Ozler, U. Alabalik, Fibroblast growth factor-1 expression in the endometrium of patients with repeated implantation failure after in vitro fertilization. *Eur. Rev. Med. Pharmacol. Sci.* **17**, 398–402 (2013).
31. E. Alan, N. Liman, H. Sağsöz, The profile of the epidermal growth factor system in rat endometrium during postpartum involution period. *Vet. Res. Commun.* **39**, 115–135 (2015).
32. E. M. Rutanen, Insulin-like growth factors in endometrial function. *Gynecol. Endocrinol. 1998* **12**, 399–406 (1998).
33. L. Zhu, J. W. Pollard, Estradiol-17β regulates mouse uterine epithelial cell proliferation through insulin-like growth factor 1 signaling. *Proc. Natl. Acad. Sci. U.S.A.* **104**, 15847–15851 (2007).
34. F. Dong, Q. Zhang, W. Kong, J. Chen, J. Ma, L. Wang, Y. Wang, Y. Liu, Y. Li, J. Wen, Regulation of endometrial cell proliferation by estrogen-induced BDNF signaling pathway. *Gynecol. Endocrinol.* **33**, 485–489 (2017).
35. I. Yotova, E. Hsu, C. Do, A. Gaba, M. Sczabolcs, S. Dekan, L. Kenner, R. Wenzl, B. Tycko, Epigenetic alterations affecting transcription factors and signaling pathways in stromal cells of endometriosis. *PLOS ONE.* **12**, e0170859 (2017).
36. J. Kroll, J. Waltenberger, Regulation of the endothelial function and angiogenesis by vascular endothelial growth factor-A (VEGF-A). *Z. Kardiol.* **89**, 206–218 (2000).
37. S. Merighi, A. Benini, P. Mirandola, S. Gessi, K. Varani, E. Leung, S. Maclennan, P. A. Borea, Adenosine modulates vascular endothelial growth factor expression via hypoxia-inducible factor-1 in human glioblastoma cells. *Biochem. Pharmacol.* **72**, 19–31 (2006).
38. X. Fan, S. Krieg, C. J. Kuo, S. J. Wiegand, M. Rabinovitch, M. L. Druzin, R. M. Brenner, L. C. Giudice, N. R. Nayak, VEGF blockade inhibits angiogenesis and reepithelialization of endometrium. *FASEB J.* **22**, 3571–3580 (2008).
39. S. K. Smith, Regulation of angiogenesis in the endometrium. *Trends Endocrinol. Metab.* **12**, 147–151 (2001).
40. Y. A. Romanov, V. A. Svintsitskaya, V. N. Smirnov, Searching for alternative sources of postnatal human mesenchymal stem cells: Candidate MSC-like cells from umbilical cord. *Stem Cells* **21**, 105–110 (2003).

Acknowledgments: We acknowledge the breeding and technical assistance of Fujian Experiment Center of Nonhuman Primate for Family Planning. We thank C. Yu for the operation of uterine D&C and open abdominal surgery. We thank C. Xiong and P. Su for their invaluable contributions in critically revising the manuscript and providing guidance for important intellectual content. We thank M. Zhang, T. Chang, and S. Song for analyzing the data and collecting the samples. **Funding:** This work was supported by the National Natural Science Foundation of China (NSFC 81571434) and the National Key Research and Development Program of China (2017YFC1002002). The funders played no role in the study design, data collection and analysis, decision to publish, or preparation of the manuscript.
Author contributions: W.X. designed the study and published this manuscript; L.W. and C.Y. performed the experiments and wrote the manuscript; M.Z., T.C., and S.S. analyzed the data and collected the samples; C.X. and P.S. provided their invaluable contributions in critically revising the manuscript and providing guidance for important intellectual content.
Competing interests: The authors declare that they have no competing interests. **Data and materials availability:** All data needed to evaluate the conclusions in the paper are present in the paper and/or the Supplementary Materials. Additional data related to this paper may be requested from the authors.

Submitted 19 December 2019
Accepted 13 March 2020
Published 22 May 2020
10.1126/sciadv.aba6357

Citation: L. Wang, C. Yu, T. Chang, M. Zhang, S. Song, C. Xiong, P. Su, W. Xiang, In situ repair abilities of human umbilical cord–derived mesenchymal stem cells and autocrosslinked hyaluronic acid gel complex in rhesus monkeys with intrauterine adhesion. *Sci. Adv.* **6**, eaba6357 (2020).